Cyano-Bridged Bimetallic Assemblies from Hexacyanometalate, $[M(CN)_6]^{3-}$ (M = Mn^{III} and Fe^{III}), and $[M(N_4\text{-macrocycle})]^{2+}$ (M = Fe^{III}, Ni^{II} and Zn^{II}) Building Blocks. Syntheses, Multidimensional Structures, and Magnetic Properties

Enrique Colacio,*,# Mustapha Ghazi,# Helen Stoeckli-Evans,† Francesc Lloret,*,‡ José María Moreno,# and Cristina Pérez#

Departamento de Química Inorgánica, Facultad de Ciencias, Universidad de Granada, 18071 Granada, Spain, Institut de Chimie, Université de Neuchâtel, Avenue de Bellevaux 51, CH-2000 Neuchâtel, Switzerland, and Departament de Química Inorgánica, Facultat de Ciencias, Universitat de Valencia, Burjassot, Valencia, Spain

Received March 28, 2001

Reactions between $[M(N_4\text{-macrocycle})]^{2+}$ (M = Zn^{II} and Ni^{II}; macrocycle ligands are either CTH = d,l-5,5,7,12,12,14-hexamethyl-1,4,8,11-tetraazacyclotetradecane or cyclam = 1,4, 8, 11-tetrazaazaciclotetradecane) and $[M(CN)_6]^{3-}$ (M = Fe^{III} and Mn^{III}) give rise to cyano-bridged assemblies with 1D linear chain and 2D honeycomblike structures. The magnetic measurements on the 1D linear chain complex $[Fe(cyclam)][Fe(CN)_6]\cdot 6H_2O$ **1** points out its metamagnetic behavior, where the ferromagnetic interaction operates within the chain and the antiferromagnetic one between chains. The Neel temperature, T_N, is 5.5 K and the critical field at 2 K is 1 T. The unexpected ferromagnetic intrachain interaction can be rationalized on the basis of the axially elongated octahedral geometry of the low spin Fe^{III} ion of the $[Fe(cyclam)]^{3+}$ unit. The isostructural substitution of $[Fe(CN)_6]^{3-}$ by $[Mn(CN)_6]^{3-}$ in the previously reported complex $[Ni(cyclam)]_3[Fe(CN)_6]_2\cdot 12H_2O$ **2** leads to $[Ni(cyclam)]_3[Mn(CN)_6]_2\cdot 16\ H_2O$ **3**, which exhibits a corrugated 2D honeycomblike structure and a metamagnetic behavior with $T_N = 16$ K and a critical field of 1 T. In the ferromagnetic phase ($H > 1$ T) this compound shows a very important coercitive field of 2900 G at 2 K. Compound $[Ni(CTH)]_3[Fe(CN)_6]_2\cdot 13H_2O$ **4**, $C_{60}H_{116}Fe_2N_{24}Ni_3O_{13}$, monoclinic, *A* 2/*n*, $a = 20.462(7)$, $b = 16.292(4)$, $c = 27.262(7)$ Å, $\beta = 101.29(4)°$, $Z = 4$, also has a corrugated 2D honeycomblike structure and a ferromagnetic intralayer interaction, but, in contrast to **2** and **3**, does not exhibit any magnetic ordering. This fact is likely due to the increase of the interlayer separation in this compound. {[Zn(cyclam)$Fe(CN)_6$Zn(cyclam)] [Zn(cyclam)$Fe(CN)_6$]$\cdot 22H_2O\cdot$EtOH} **5**, $C_{44}H_{122}Fe_2N_{24}O_{23}Zn_3$, monoclinic, *A* 2/*n*, $a = 14.5474(11)$, $b = 37.056(2)$, $c = 14.7173(13)$ Å, $\beta = 93.94(1)°$, $Z = 4$, presents an unique structure made of anionic linear chains containing alternating $[Zn(cyclam)]^{2+}$ and $[Fe(CN)_6]^{3-}$ units and cationic trinuclear units $[Zn(cyclam)Fe(CN)_6Zn(cyclam)]^+$. Their magnetic properties agree well with those expected for two $[Fe(CN)_6]^{3-}$ units with spin−orbit coupling effect of the low spin iron(III) ions.

Introduction

In recent years considerable research has been put into the design and elaboration of new polymetallic molecular materials with extended structures which have intriguing properties and potential applications in catalysis, electrical conductivity, molecular-based magnets, and host−guest chemistry.[1,2] A useful and popular approach for this purpose consists of assembling two building blocks that frequently are transition metal complexes, one with terminal ligands capable of acting as bridges and another with empty or available co-oordination sites. A typical example of paramagnetic ligands than can be used for this purpose is the family of cyanometalate complexes,[3] which react with transition metal aqua complexes to afford 3D cyanide-bridged bimetallic assemblies of Prussian-blue type.[4] These materials exhibit spontaneous magnetization at considerable high

* To whom correspondence should be addressed.
# Universidad de Granada.
† Université de Neuchâtel.
‡ Universitat de Valencia.

(1) (a) *Magnetic Molecular Materials*; Gatteschi, D., O. Kahn, O., Miller, J. S., Palacio, F., Eds.; NATO ASI Series E198; Kluwer Academic Publishers: Dordrecht, The Nederlands, 1991. (b) *Magnetism: A Supramolecular Function*; Kahn, O., Ed.; NATO ASI Series C484; Kluwer Academic Publishers: Dordrecht, The Nederlands, 1996. (c) *Molecular Magnetism: From the Molecular Assemblies to the Devices*; Coronado, E., Delhaés, P., Gatteschi, D., Miller, J. S., Eds.; NATO ASI Series E321; Kluwer Academic Publishers: Dordrecht, The Nederlands, 1996. (d) *Research Frontiers in Magnetochemistry*; O'Connor, C. J., Ed.; World Scientific Publishing Co. Pte. Ltd.: Singapore, 1993. (e) Kahn, O. *Adv. Inorg. Chem.* **1995**, *43*, 179. (f) Kahn, O. *Molecular Magnetism*; VCH: New York, 1993. (f) Coronado, E.; Galán-Mascarós, J. R.; Gómez-García, C. J.; Laukhin, V. *Nature* **2000**, *408*, 447.

(2) Robson, R.; Abraham, B. F.; Batten, S. R.; Gable, R. W.; Hoskins, B. F.; Liu J. In *Supramolecular Architecture*; Bein, T., Ed.; American Chemical Society: Washington, DC, 1992; Chapter 19, p 258. Robson, R. In *Comprehensive Supramolecular Chemistry*; Pergamon: New York, 1996, Chapter 22, p 733. Batten S. R.; Robson, R. *Angew. Chem., Int. Ed. Engl.* **1998**, *37*, 1460. Subramanian, S.; Zaworotko, M. J. *Angew. Chem., Int. Ed. Engl.* **1995**, *34*, 2127. Zaworotko, M. J.; Rogers, R. D. In *Synthesis of New Materials by Coordination Chemistry Self-Assembly and Template Formation*, 1999. Yaghi, O. M.; Li, G.; Li, H. *Nature* **1995**, *378*, 703. Yaghi O. M.; Li, H.; Groy, T. L. *J. Am. Chem. Soc.* **1996**, *118*, 9096. Yaghi O. M.; Li, H. *J. Am. Chem. Soc.* **1995**, *117*, 10401. Yaghi O. M.; Li, H. *J. Am. Chem. Soc.* **1996**, *118*, 295. Kondo M.; Okubo, T.; Asami, A.; Noro, S.; Yoshimoto, T.; Kitagawa, S.; Ishii, T.; Matsuzaka, H.; Seki, K. *Angew. Chem., Int. Ed. Engl.* **1999**, *38*, 140. Fujita, M.; Kwon, Y. J.; Washizu, S.; Ogura, K. *J. Am. Chem. Soc.* **1994**, *116*, 1151.

(3) Dumbar, K. R.; Heintz, R. A. *Prog. Inorg. Chem.* **1997**, *45*, 283.

10.1021/ic0103446 CCC: $20.00
Published on Web 08/16/2001

temperatures and interesting electrochemical, optoelectronic and magnetooptical properties.[3−5] The crystallization of the Prussian-blue analogues, however, is very difficult and then structural information is very limited.[6] One alternative route to bimetallic cyanide-bridged materials is that of assembling cyanometalate building blocks $[M(CN)_n]^{m-}$ (M = Mo(V), W(V), $n = 8$; M = Mo(III), $n = 7$; M = Cr(III), Fe(III), Co(III), and Fe(II), $n = 6$) and coordinatively unsaturated metal complexes with polydentate ligands blocking selected positions. This strategy favors the crystallization and then the magneto-structural study. Depending of the nature of the building blocks, different and fascinating structures, that range from discrete entities to 3D extended networks, can be obtained, some of which exhibit interesting magnetic properties, such as magnetic ordering and ground spin states as high as $S = 51/2$.[7−27]

In this context, recently, we have explored the assembling reactions between $[M(cyclam)]^{2+}$ (M = Ni(II) and Cu(II); cyclam = 1,4, 8, 11-tetrazaazaciclotetradecane) and $[Fe(CN)_6]^{3-}$ building blocks.[7−10] From $[Ni(cyclam)]^{2+}$ two different cyanide-bridged complexes were obtained depending on the molar ratio of the reactants, $[Fe(cyclam)][Fe(CN)_6]\cdot 6H_2O$ **1**[8] and $[Ni(cyclam)]_3[Fe(CN)_6]_2\cdot 12H_2O$ **2**.[7] The former exhibits a 1D chain structure with alternating iron(III) sites and unexpected ferromagnetic coupling within the chain, whereas the latter has a 2D honeycomblike layered structure and exhibits a metamagnetic behavior derived from ferromagnetic intralayers and weak antiferromagnetic interlayers interactions. Furthermore, below 3 K a canted structure is formed leading to a ferromagnetic ordering. In this paper we have carried out a deep magnetic study on the $[Fe(cyclam)][Fe(CN)_6]\cdot 6H_2O$ **1** in order to gain insight into its magnetic behavior in the low-temperature regime. In addition, we report here on the magnetic properties of the complex $[Ni(cyclam)]_3[Mn(CN)_6]_2\cdot 16H_2O$ **3**, which is prepared by isostructural substitution in the complex $[Ni(cyclam)]_3[Fe(CN)_6]_2\cdot 12H_2O$ of $[Fe(CN)_6]^{3-}$ by $[Mn(CN)_6]^{3-}$, a building block with relevant anisotropy and more t_{2g} unpaired electrons than $[Fe(CN)_6]^{3-}$. Finally, the syntheses, structure and magnetic properties of the complexes $[Ni(CTH)]_3[Fe(CN)_6]_2\cdot 12H_2O$ **4** (CTH = d,l-5,5,7,12,12,14-hexamethyl-1,4,8,11-tetrazacyclotetradecane) and {[Zn(cyclam)Fe(CN)$_6$Zn(cyclam)] [Zn(cyclam)-Fe(CN)$_6$]$\cdot 22H_2O\cdot$EtOH} **5** are also reported. With the former, which exhibits a similar structure to $[Ni(cyclam)]_3[Fe(CN)_6]_2\cdot 12H_2O$, we intend to investigate the effect of bulkier substituents on the macrocyclic ligand on the interlayer antiferromagnetic interactions. Complex **5** presents an unique structure made of anionic linear chain containing alternating $[Zn(cyclam)]^{2+}$ and $[Fe(CN)_6]^{3-}$ units and cationic trinuclear units [Zn(cyclam)Fe(CN)$_6$Zn(cyclam)]$^+$.

(4) Verdaguer, M. *Science* **1996**, *272*, 698. Entley, W.; Girolami, G. S. *Science* **1995**, *268*, 397. (b) Kahn, O. *Nature* **1995**, *378*, 667. (c) Ferlay, S.; Mallah, T.; Ouahes, R.; Veillet, P.; Verdaguer, M. *Nature* **1995**, *378*, 701. Verdaguer, M.; Bleuzen, A.; Marvaud, V.; Vaissermann, J.; Seuleiman, M.; Desplanches, C.; Scuiller, A.; Train, C.; Garde, R.; Gelly, G.; Lomenech, C.; Rosenman, I.; Veillet, P.; Cartier, C.; Villain, F. *Coord. Chem. Rev.* **1999**, *190*. 1023.

(5) (a) Sato, O.; Iyoda, T.; Fujishina, A.; Hashimoto, K. *Science* **1996**, *271*, 46. (b) Sato, O.; Iyoda, T.; Fujishina, A.; Hashimoto, K. *Science* **1996**, *272*, 704.

(6) Ludi, A.; Güdel, H. U. *Struct. Bonding (Berlin)* **1973**, *14*, 1.

(7) Colacio, E.; Domínguez-Vera, J. M.; Ghazi, M.; Kivekäs, R.; Lloret, F.; Moreno, J. M.; Stoeckli-Evans, H. *J. Chem. Soc. Chem. Commun.* **1999**, 987.

(8) Colacio, E.; Domínguez-Vera, J. M.; Ghazi, M.; Kivekäs, R.; Klinga M.; Moreno, J. M. *J. Chem. Soc., Chem. Commun.* **1998**, 1071.

(9) Colacio, E.; Domínguez-Vera, J. M.; Ghazi, M.; Kivekäs, R.; Moreno, J. M.; Pajunen, A. *J. Chem. Soc., Dalton Trans.* **2000**, 509.

(10) Colacio, E.; Domínguez-Vera, J. M.; Ghazi, M.; Kivekäs, R.; Lloret, F.; Moreno, J. M.; Stoeckli-Evans, H. *Mol. Cryst. and Liq. Cryst*. **1999**, *335*, 283.

(11) Kou, H.-Z.; Gao, S.; Bu, W.-M.; Liao, D.-Z.; Ma, B.-Q.; Jiang, Z.-H.; Yan, S.-P.; Fan, Y.-G.; Wang, G.-L. *J. Chem. Soc., Dalton Trans.* **1999**, 2477. Kou, H.-Z.; Gao, S.; Ma, B.-Q.; Liao, D.-Z. *J. Chem. Soc., Chem. Commun.* **2000**, 713. Kou, H.-Z.; Liao, D.-Z.; P. Cheng, Z.-H. Jiang, S.-P. Yan, G. L. Wang, X.-K. Yao H.-G. Wang, *J. Chem. Soc., Dalton Trans.* **1997**, 1503. Kou, H.-Z.; Bu, W.-M.; Liao, D.-Z.; Cheng, P.; Jiang, Z.-H, Yan, S.-P.; Fan Y.-G.; Wang, G.-L. *J. Chem. Soc., Dalton Trans.* **1998**, 4161. Kou, H.-Z.; Gao, S.; Liao, D.-Z.; Jiang, Z.-H.; Yan, S.-P.; Fan, Y.-G.; Wang, G.-L. *J. Chem. Soc., Dalton Trans.* **2000**, 2996.

(12) Kou, H.-Z.; Gao, S.; Ma, B.-Q.; Liao, D.-Z. *J. Chem. Soc., Chem. Commun.* **2000**, 1309.

(13) Ferlay, S.; Mallah, T.; Vaisserman, J.; Bartolomé, F.; Veillet P.; Verdaguer, M. *J. Chem. Soc., Chem. Commum*. **1996**, 2481. Mallah, T.; Auberger, C.; Verdaguer M.; Veillet, P. *J. Chem. Soc., Chem. Commun.* **1995**, 61; Scuiller, A.; Mallah, T.; Verdaguer, M.; Nivorozkhin, A.; Tholence J.; Veillet, P. *New J. Chem.* **1996**, *20*, 1. Marvilliers, A.; Pei, Y.; CanoBoquera-J.; Vostrikova, K. E., Paulsen, E.; Riviere, E.; Audiére J. P.; Mallah, T. *J. Chem. Soc., Chem. Commun.* **1999**, 1951. Marvilliers, A.; Mallah, T.; Parsons, S.; Muñoz, C.; Vostrikova, K. E. *Mol. Cryst. and Liq. Cryst.* **1999**, *335*, 1195. Rogez, G.; Marvilliers, A.; Riviere, E.; Audiére J. P.; Lloret, F.; Varret, F.; Goujon, A.; Menendez, N.; Girerd, J. J.; Mallah, T. *Angew. Chem., Int. Ed.* **2000**, *39*, 2885.

(14) Miyasaka, H.; Matsumoto, N.; Okawa, H.; Re, N.; Gallo, E.; Floriani, C. *J. Am. Chem. Soc.* **1996**, *118*, 981. Miyasaka, H.; Matsumoto, N.; Re, N.; Gallo, E.; Floriani, C. *Inorg. Chem.* **1997**, *36*, 670. Re, N.; Crescenzi, R.; Floriani, C.; Miyasaka, H.; Matsumoto, N. *Inorg. Chem.* **1998**, *37*, 27 17. Re, N.; Gallo, E.; Floriani, C.; Miyasaka, H.; Matsumoto, N. *Inorg. Chem.* **1996**, *35*, 6004.

(15) Ohba, M.; Okawa, K. *Coord. Chem. Rev.* **2000**, *198*, 313 and references therein.

(16) Fu, D. G.; Chen, J.; Tan, X. S.; Jiang, L. J.; Zhang, S. W.; Zheng, P. J.; Tang, W. X. *Inorg. Chem.* **1997**, *36*, 220.

(17) Salah El Fallah, M.; Rentschler, E.; Caneschi, A.; Sessoli R.; Gatteschi, D. *Angew. Chem., Int. Ed. Eng.* **1996**, *35*, 9047.

(18) Parker, R. J.; Hockless, D. C.; Moubaraki, B.; Murray, K. S.; Spiccia, L. *J. Chem. Soc., Chem. Commun.* **1996**, 2789. Langenberg K. V.; Batten S. R.; Berry, K. J.; Hockless D. C. R.; Moubaraki B.; Murray K. S. *Inorg. Chem.* **1997**, *36*, 5006.

(19) Lu, Z.-L.; Duan, C.-Y.; Tian, Y.-P.; Wu, Z.-W.; You, J.-J.; Zhou, Z.-Y.; Mak, T. C. W. *Polyhedron* **1997**, *16*, 909.

(20) Morpurgo, G. O.; Mosini, V.; Porta, P.; Dessy, G.; Fares, V. *J. Chem. Soc., Dalton Trans.* **1980**, 1272.

(21) Larionova, J.; Sanchiz, J.; Golhen, S.; Ouahab, L.; Kahn, O. *J. Chem. Soc. Chem. Commun.* **1998**, 953. Larionova, J.; Clérac R.; Sanchiz, J.; Kahn, O.; Golhen, S.; Ouahab, L. *J. Am. Chem. Soc.* **1998**, *120*, 13088. Larionova, J.; Kahn, O.; Golhen, S.; Ouahab, L.; Clérac R. *J. Am. Chem. Soc.* **1999**, *121*, 3349. Rombaut, G.; Golhen, S.; Ouahab, L.; Manthonière, C.; Khan O. *J. Chem. Soc., Dalton Trans.* **2000**, 3609. Sra, A. K.; Andruh, M.; Khan, O.; Golhen, S.; Ouahab, L.; Yakhmi, J. V. *Angew. Chem., Int. Ed*. **1999**, *38*, 2606. Larionova, J.; Kahn, O.; Bartolome, J.; Burriel, R.; Castro, M.; Ksenofontov, V.; Gutlich; P. *Chem. Mater*. **1999**, *11*, 3400. Khan, O. *Philos. Trans. Royal. Soc. London, Ser*. A **1999**, *357*, 1762. Larionova, J.; Kahn, O.; Golhen, S.; Ouahab, L.; Clérac, R. *Inorg. Chem.* **1999**, *38*, 3621. Khan, O.; Larionova, J.; Ouahab, L. *J. Chem. Soc. Chem. Commun.* **1999**, 945. Rombaut, G.; Golhen, S.; Ouahab, L.; Manthonière, C.; Khan O. *J. Chem. Soc., Dalton Trans.* **2000**, 3609. Tanase, S.; Ferbinteaunu, M.; Andruh M.; Mathionere C.; Strenger, I.; Rombaut, G. *Polyhedron* **2000**, *19*, 1967.

(22) Larionova, J.; Gross, M.; Pilkington, M.; Andres, H.; Stoeckli-Evans, H.; Güdel, U.; Decurtins, S. *Angew. Chem., Int. Ed. Eng.* **1996**, *35*, 9047.

(23) Zhong, Z. J.; Seino, H.; Mozobe, Y.; Hidai, M.; Fujishima, A.; Ohkoski, S.; Hashomoto, K. *J. Am. Chem. Soc.* **2000**, *122*, 2952. Zhong, Z. J.; Seino, H.; Mizobe, Y.; Hidai, M.; Verdaguer, M.; Ohkoshi, S.; Hashimoto, K. *Inorg. Chem.* **2000**, *39*, 5095.

(24) Heinrich, J. L.; Berseth, P. A.; Long, J. R. *Chem. Commun.* **1998**, 1231.

(25) Clemente-León, M.; Coronado, E.; Galán-Mascarós, J. R.; Gómez-García, C. J.; Canadell, E. *Inorg. Chem.* **2000**, *24*, 5394. Smith, J. A.; Galán-Mascarós, J. R.; Clerac, R.; Dunbar, K. R. *J. Chem. Soc., Chem. Commun*. **2000**, *12*, 1077.

(26) Bernhardt, P. V.; Macpherson, B. P.; Martínez, M. *Inorg. Chem.* **2000**, *24*, 5203.

(27) Mondal, N.; Saha, M. K.; Bag, B.; Mitra, S.; Gramlich, V.; Ribas, J.; Salah El Fallah, M. *J. Chem. Soc., Dalton* **2000**, 1601.

Experimental Section

Physical Measurements. Elemental analyses were carried out at the Centro de Instrumentación Científica of the University of Granada on a Fisons-Carlo Erba analyzer model EA 1108. IR spectra were recorded on a MIDAC model Progress-IR spectrometer using KBr pellets. Variable-temperature magnetic susceptibility data were collected on powdered samples of the compounds with use of a SQUID-based sample magnetometer on a Quantum Design Model MPMS instrument. Data were corrected for the diamagnetism of the ligands using Pascal's constants. X-ray diffraction patterns of powdered samples were recorded on a Phillips PW1700 diffractometer with a graphite monochromator and Cu Kα radiation ($\lambda = 1.54051$ Å).

Caution! Perchlorate complexes of metal ions are potentially explosive. Only a small amount of material should be handled with caution.

Preparations of the Compounds. $[Ni(CTH)][ClO_4]_2$, $[Ni(cyclam)][ClO_4]_2$, and $K_3[Mn(CN)_6]$ were prepared by literature methods.[28,29,30] Complex **2** was prepared as previously we reported.[7]

$[Fe(cyclam)][Fe(CN)_6]\cdot 6H_2O$ 1. To an aqueous solution of $[Ni(cyclam)](ClO_4)_2$ (0.10 g, 0.22 mmol) in 50 cm^3 of water was added a large amount of $K_3[Fe(CN)_6]$ (0.73 g, 2.2 mmol). The resulting dark brown solution kept at room temperature for several days, afforded dark green crystals which were filtered and air-dried. Yield: 73%. Anal. Calcd for $C_{16}H_{36}N_{10}O_6Fe_2$: C, 33.32; H, 6.30, N 24.30. Found: C, 33.29; H 6.38; N 24.04. IR(KBr): ν(CN), 2151, 2125 cm^{-1}. Although this compound can also be prepared from $K_3[Fe(CN)_6]$ and cyclam in hydroethanolic medium the yield is very poor.

$[Ni(cyclam)]_3[Mn(CN)_6]_2\cdot 16H_2O$ 3. To an ice-cooled solution of $[Ni(cyclam)](ClO_4)_2$ (0.10 g, 0.22 mmol) in 30 cm^3 of water was added with stirring an ice-cooled solution of $K_3[Mn(CN)_6]$ (0.072 g, 0.22 mmol, 0.07 g) in 15 cm^3 of water. A brown precipitate was obtained, which was filtered off, washed with water and air-dried. Yield: 70%. Anal. Calcd for $C_{42}H_{104}N_{24}O_{16}Mn_2Ni_3$: C, 33.93; H, 6.99, N 22.61. Found: C, 33.87; H 6.42; N 21.99. IR(KBr): ν(CN), 2116, 2139 cm^{-1}.

$[Ni(CTH)]_3[Fe(CN)_6]_2\cdot 13H_2O$ 4. To an aqueous solution of $[Ni(CTH)][ClO_4]_2$ (0.10 g, 0.21 mmol) in 20 cm^3 of water was added $K_3[Fe(CN)_6]$ (0.067 g, 0.21 mmol) in 15 cm^3 of water with continuous stirring at room temperature. The brown precipitate thus produced was collected by filtration, washed with water and air-dried. Yield: 85%. Anal. Calcd for $C_{60}H_{107}N_{24}O_{13}Fe_2Ni_3$: C, 43.45; H, 6.46, N 20.28. Found: C, 43.33; H 6.72; N 20.38. IR(KBr): ν(CN), 2115, 2143 cm^{-1}. Crystals for X-ray analysis were obtained by slow diffusion of two aqueous solutions of the reactans into a U-tube containing agarose gel.

{$[Zn(cyclam)Fe(CN)_6Zn(cyclam)][Zn(cyclam)Fe(CN)_6]\cdot 22H_2O\cdot$ EtOH} 5. To a solution of cyclam (0.097 g, 0.48 mmol) in 15 cm^3 of ethanol was added $Zn(NO_3)_2\cdot 6H_2O$ (0.14 g, 0.48 mmol) in 10 cm^3 of ethanol and then an aqueous solution of $K_3[Fe(CN)_6]$ (0.1 g, 0.3 mmol). A yellow precipitate was obtained, which was filtered-off, washed with ethanol and air-dried. Yield: 85%. Anal. Calcd for $C_{44}H_{102}N_{24}O_{23}Zn_3Fe_2$: C, 35.63; H, 6.88, N 22.67. Found: C, 35.79; H 6.78; N 23.12. IR(KBr): ν(CN), 2110, 2123 cm^{-1}. Yellow needles-like crystals suitable for X-ray analysis were obtained by slow evaporation of the filtrate. IR spectra and X-ray powder diffractograms clearly indicate that crystals and polycrystalline samples of **5** are the same compound.

Crystallography. The intensity data for suitable crystals of compounds **4** (very thin brown plate) and **5** (brown-yellow plate) were collected at 203 K and 223 K, respectively, on a Stoe Image Plate Diffraction System[31] using Mo Kα graphite monochromated radiation. Image plate distance 70 mm, ϕ scans 0−200°, step $\Delta\phi = 1°$, 2θ range 3.27−52.1°, $d_{max} - d_{min} = 12.45-0.8$ 1 Å. The structure was solved by direct methods using SHELXS-97.[32] The refinement and all further calculations were carried out using SHELXL-97.[33] The crystal of compound **4** diffracted very poorly, only out to 40° in 2θ (average $I/\sigma(I)$ ca. 1.5). The CTH molecules were also disordered. For compound **5** the H-atoms of the cyclam rings were included in calculated positions and treated as riding atoms using SHELXL-97 default parameters. For **4** only the zinc, iron and N-atoms were refined anisiotropically and no H-atoms were included, while for **5** all the non-H atoms were refined anisotropically, using weighted full-matrix least-squares on F^2. Crystal data and details of the data collection and refinement for **4** and **5** are summarized in Table 1.

Table 1. Crystallographic Data for **4** and **5**

	4	**5**
chemical formula	$C_{60}H_{116}Fe_2N_{24}Ni_3O_{13}$	$C_{44}H_{122}Fe_2N_{24}O_{23}Zn_3$
formula weight	1669.60	1663.47
space group	*A* 2/*n*	*A* 2/*n*
a, Å	20.462(7)	14.5474(11)
b, Å	16.292(4)	37.056(2)
c, Å	27.262(7)	14.7173(13)
α, deg	90	90
β, deg	101.29(4)	93.94(1)
γ, deg	90	90
V, Å^3	8912(4)	7914.8(11)
Z	4	4
λ, Å	0.71073	0.71073
ρ_{calcd}, g cm^{-3}	1.244	1.396
μ, mm^{-1}	1.003	1.332

[a] $R = \sum||F_o| - |F_c||/\sum|F_o|$. [b] $R_w = (\sum[w(F_o^2 - F_c^2)^2])/\sum[w(F_o^2)^2])^{1/2}$. $w = q/[\sigma^2(F_o^2) + (a*P)^2 + b*P + d + e*\sin(\theta)]$.

Results and Discussion

As indicated elsewhere, when a large excess of $[Fe(CN)_6]^{3-}$ with regard to $[Ni(cyclam)]^{2+}$ is used, the Ni^{II} ion of the $[Ni(cyclam)]^{2+}$ unit is substituted by Fe^{III} and the compound $[Fe(cyclam)][Fe(CN)_6]\cdot 6H_2O$ **1** is obtained. Its structure[8] consists of neutral polymeric linear chains of alternated $[Fe(cyclam)]^{3+}$ and $[Fe(CN)_6]^{3-}$ ions, in which two CN^- groups of each $[Fe(CN)_6]^{3-}$ unit in *trans* positions bridge two iron (III) atoms (see Figure 1). From the same building blocks, $[Fe(CN)_6]^{3-}$ and $[Ni(cyclam)]^{2+}$, but using a 1:1 molar ratio the complex $[Ni(cyclam)]_3[Fe(CN)_6]_2\cdot 12H_2O$ **2** is formed. It exhibits a corrugated 2D honeycomblike structure,[7] in which each $[Fe(CN)_6]^{3-}$ is coordinated through cyanide bridges to three $[Ni(cyclam)]^{2+}$ in a *fac* arrangement, whereas each $[Ni(cyclam)]^{2+}$ cation is linked to two $[Fe(CN)_6]^{3-}$ units in *trans* positions (see Figure 1). Water molecules occupy the interlayer space and are linked to terminal CN^- groups of the $[Fe(CN)_6]^{3-}$ units and to other water molecules by hydrogen bonds. The isostructural substitution of $[Fe(CN)_6]^{3-}$ by $[Mn(CN)_6]^{3-}$ in **2**, leads to $[Ni(cyclam)]_3[Mn(CN)_6]_2\cdot 16\ H_2O$ **3**. The IR spectra and X-ray diffraction patterns of **2** and **3** (Figure 2) are very similar, almost identical, indicating that these complexes have the same two-dimensional framework, although the interlayer spacing may be different.

Compound **4** was prepared from $[Ni(CTH)]^{2+}$ and $[Fe(CN)_6]^{3-}$ building blocks. Crystals of **4** were not of enough quality as to solve the structure with high degree of accuracy ($R = 0.13$). Nevertheless, at this level of solution there is not any doubt about the more relevant features of this compound. Thus, its structure is very similar to that of **2** and consists of corrugated 2D honeycomblike layers and water molecules between layers. In the crystals, layers align along *a* axis with an interlayer separation of ca. 10.03 Å, which is longer than that observed for **2** of 8.968 Å. The increase of the interlayer spacing in **4** is likely due the presence of bulkier substituents, methyl groups,

(28) Curtis, N. F.; Swann, D. A.; Waters, T. N. *J. Chem. Soc., Dalton Trans*. **1973**, 1963.
(29) Bosnich, B.; Tobe, M. L.; Webb, G. A. *Inorg. Chem*. **1965**, *4*, 1109.
(30) Lower, J. A.; Fernelius, W. C. *Inorg. Synthesis* **1949**, *2*, 213.
(31) Stoe Cie 2000. *IPDS Software*. Stoe & Cie GmbH: Darmstadt, Germany.
(32) Sheldrick, G. M. "SHELXS-97, Program for Crystal Structure Determination" *Acta Crystallogr*. **1990**, *A46*, 467.
(33) Sheldrick, G. M. *SHELXL-97*; Universität Göttingen: Göttingen, Germany, 1999.

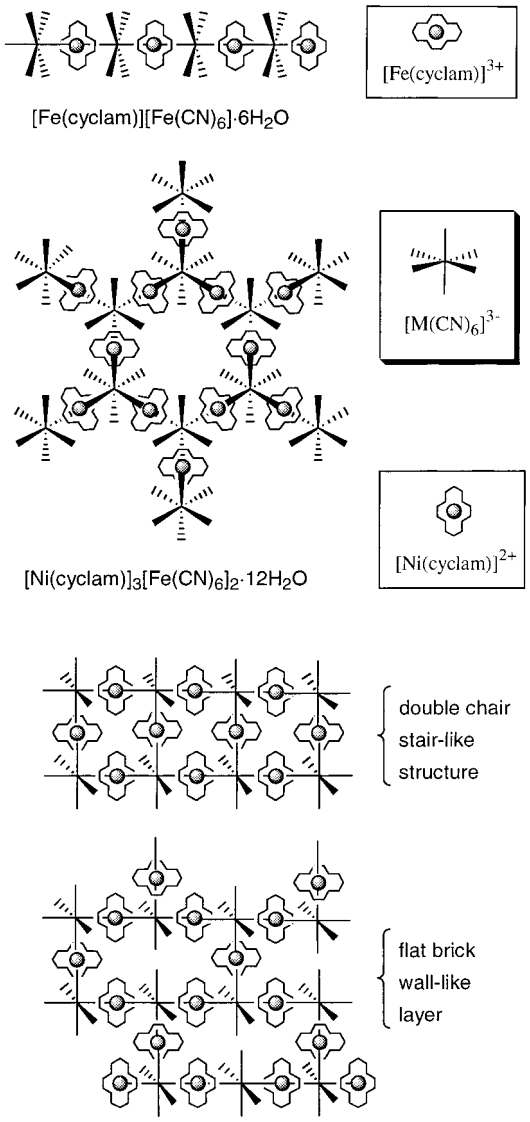

Figure 1. Scheme of the crystal structures of **1** and **2** (top) and a plot of 2D flat brick wall-like layer and double chain stair like arrangements (bottom).

on the macrocycle. Furthermore, each layer is shifted also along *b* axis with respect to the neighboring layers in order to relieve steric crowding, giving rise to a ABAB... layer sequence. Relevant bond distances and angles are gathered in Table 2.

From $[Zn(cyclam)]^{2+}$ and $[Fe(CN)_6]^{3-}$ building blocks compound 5, a Zn_3Fe_2 system, was obtained. For cyanide-bridged $M_3M'_2$ systems containing *trans* M^{II}−macrocyclic complexes, when coordination positions on the M^{II} ion are fully saturated, three different structures are possible depending on the arrangement of M^{II}−macrocyclic units around the M′ ion. Thus, a facial arrangement leads to a corrugated 2D honeycomblike structure, like that of **2**−**4**, whereas a meridional arrangement leads to either a 2D flat brick wall-like layer[12] or a double chain stair-like structure[15] (Figure 1). Nevertheless, if the M^{II} of the macrocyclic-complex unit can exhibit two coordination numbers, five and six, a new structural type, that of **5**, can be obtained. Its unique structure consists of polymeric anionic chains of alternating $[Zn(cyclam)]^{2+}$ and $[Fe(CN)_6]^{3-}$ units along the crystallographic *c* axis, cationic trinuclear entities, $[Zn(cyclam)\text{-}Fe(CN)_6Zn(cyclam)]^{+}$, water molecules and a molecule of ethanol. A perspective view of a chain and a trinuclear cation, with the atom labeling scheme, is given in Figure 3, whereas selected bond lengths and angles are gathered in Table 2. Within

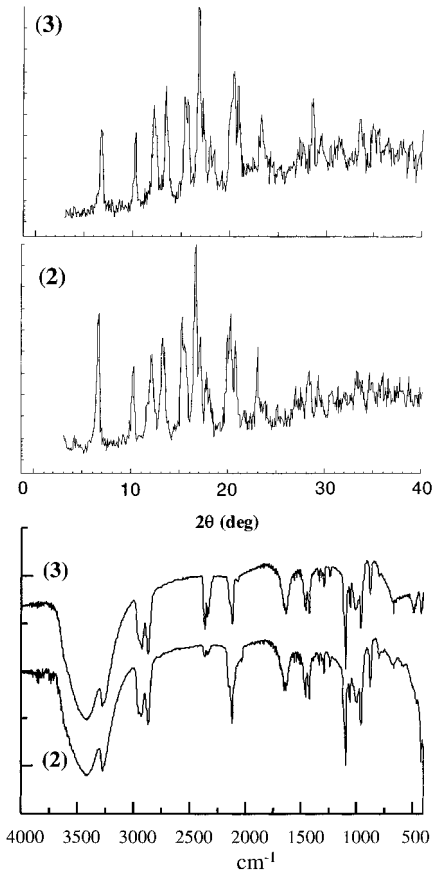

Figure 2. Powder X-ray diffractiograms (top) and IR spectra (bottom) for **2** and **3**.

the chains, similar to those observed for 1 and $K[Cu(cyclam)]\text{-}[Fe(CN)_6]\cdot 4H_2O$,[9] two CN^- groups of each $[Fe(CN)_6]^{3-}$ unit bridge two Zn(II) atoms with an $Fe^{III}\cdots Zn^{II}$ distance of 5.349 Å. The Zn(II) ion, which is located on a center of symmetry, assumes an axially distorted octahedral ZnN_6 coordination polyhedron, with the nitrogen atoms of the cyanide bridging groups occupying the axial positions. The iron center in the $[Fe(CN)_6]^{3-}$ unit, as usual, adopts a minimally distorted octahedral environment. The Fe−C−N and Zn−N−C bond angles for bridging cyanide groups of 176.6(3)° and 158.3(3)°, respectively, indicates that chains are slightly deviated from linearity.

Trinuclear units are made of two $[Zn(cyclam)]^{2+}$ units linked to a minimally distorted octahedral $[Fe(CN)_6]^{3-}$ unit in *trans* positions, leading to an Fe(III)···Zn(II) distance of 5.053 Å.The Fe−C−N and Zn−N−C bond angles for bridging cyanide groups of 177.6(3)° and 158.7(3)° are very similar to those observed for the chain. The ZnN_5 chromophore exhibits a square-pyramidal geometry wit a τ factor value of 0.001 (τ = 0 for a square-pyramid and $\tau = 1$ for trigonal bipyramid).[34] In this description, the nitrogen atoms of the macrocyclic ligand occupy the basal positions, whereas the nitrogen atom of the cyanide bridging group occupies the axial position at a longer distance. Chains, trinuclear units, water and ethanol molecules are joined by an extended network of hydrogen bonds involving the NH groups of the macrocyclic ligands, nitrogen atoms of terminal cyanide groups, water and ethanol molecules.

Magnetic Properties. As indicated above, in a previous paper[8] we reported the temperature dependence of the $\chi_M T$

(34) Addison, A. W.; Rao, T. N.; Reedijk, J.; van Riju, J.; Verschoor, G. C. *J. Chem. Soc., Dalton Trans.* **1984**, 1349.

Table 2. Bond Lengths [A] and Angles [deg] for **4** and **5**

Complex **4**			
Fe(1)−C(29)	1.70(5)	Fe(1)−C(32)	1.81(7)
Fe(1)−C(30)	2.00(4)	Fe(1)−C(33)	2.03(4)
Fe(1)−C(31)	1.93(3)	Fe(1)−C(34)	1.91(4)
Ni(1)−N(1)	2.11(3)	Ni(1)−N(4)	2.03(3)
Ni(1)−N(2)	2.07(3)	Ni(1)−N(7)	2.11(5)
Ni(1)−N(3)	2.05(2)	Ni(1)−N(8)	2.17(5)
Ni(2)−N(5)	2.15(3)	Ni(2)−N(5)^{i}	2.15(3)
Ni(2)−N(6)	2.10(4)	Ni(2)−N(6)^{i}	2.10(4)
Ni(2)−N(9)	2.11(3)	Ni(2)−N(9)^{i}	2.11(3)
C(29)−Fe(1)−C(32)	175(3)	C(34)−Fe(1)−C(30)	176.0(14)
C(31)−Fe(1)−C(33)	171.0(17)	N(4)−Ni(1)−N(2)	177.5(14)
N(3)−Ni(1)−N(1)	177.0(16)	N(7)−Ni(1)−N(8)	177.2(16)
N(9)−Ni(2)−N(9)^{i}	179(2)	N(6)^{i}−Ni(2)−N(5)	175.8(13)
N(6)−Ni(2)−N(5)^{i}	175.8(13)		

$i = -x + {}^{1}/_{2}, y, -z + {}^{1}/_{2}$

Complex **5**			
Zn(1)−N(1)	2.084(5)	Zn(1)−N(2)	2.108(5)
Zn(1)−N(3)	2.100(5)	Zn(1)−N(4)	2.089(5)
Zn(1)−N(5)	2.078(3)	Zn(2)−N(6)	2.098(5)
Zn(2)−N(7)	2.071(4)	Zn(2)−N(8)	2.365(3)
Fe(1)−C(16)	1.913(7)	Fe(1)−C(17)	1.948(4)
Fe(1)−C(18)	1.931(8)	Fe(1)−C(19)	1.932(3)
Fe(2)−C(20)	1.945(4)	Fe(2)−C(21)	1.934(7)
Fe(2)−C(22)	1.939(7)	Fe(2)−C(23)	1.952(3)
N(5)−Zn(1)−N(1)	99.3(2)	N(5)−Zn(1)−N(4)	99.0(2)
N(1)−Zn(1)−N(4)	95.66(16)	N(5)−Zn(1)−N(3)	97.1(2)
N(1)−Zn(1)−N(3)	163.45(14)	N(4)−Zn(1)−N(3)	84.23(17)
N(5)−Zn(1)−N(2)	97.16(19)	N(1)−Zn(1)−N(2)	84.74(17)
N(4)−Zn(1)−N(2)	163.55(14)	N(3)−Zn(1)−N(2)	90.74(14)
N(7)−Zn(2)−N(7)^{ii}	180.00(16)	N(7)−Zn(2)−N(6)	85.20(14)
N(7)^{ii}−Zn(2)−N(6)	94.80(14)	N(7)−Zn(2)−N(6)^{ii}	94.80(14)
N(7)^{ii}−Zn(2)−N(6)^{ii}	85.20(14)	N(6)−Zn(2)−N(6)^{ii}	180.00(17)
N(7)−Zn(2)−N(8)	91.11(16)	N(7)^{ii}−Zn(2)−N(8)	88.89(16)
N(6)−Zn(2)−N(8)	88.07(17)	N(6)^{ii}−Zn(2)−N(8)	91.93(17)
N(7)−Zn(2)−N(8)^{ii}	88.89(16)	N(7)^{ii}−Zn(2)−N(8)^{ii}	91.11(16)
N(6)−Zn(2)−N(8)^{ii}	91.93(17)	N(6)^{ii}−Zn(2)−N(8)^{ii}	88.07(17)
N(8)−Zn(2)−N(8)^{ii}	180.0	C(16)−Fe(1)−C(18)	180.000(1)
C(16)−Fe(1)−C(19)^{i}	90.00(13)	C(18)−Fe(1)−C(19)^{i}	90.00(13)
C(16)−Fe(1)−C(19)	90.00(13)	C(18)−Fe(1)−C(19)	90.00(13)
C(19)^{i}−Fe(1)−C(19)	180.0(3)	C(16)−Fe(1)−C(17)^{i}	90.02(18)
C(18)−Fe(1)−C(17)^{i}	89.98(18)	C(19)^{i}−Fe(1)−C(17)^{i}	89.74(14)
C(19)−Fe(1)−C(17)^{i}	90.26(14)	C(16)−Fe(1)−C(17)	90.02(18)
C(18)−Fe(1)−C(17)	89.98(18)	C(19)^{i}−Fe(1)−C(17)	90.26(14)
C(19)−Fe(1)−C(17)	89.74(14)	C(17)^{i}−Fe(1)−C(17)	180.0(4)
C(21)−Fe(2)−C(22)	180.000(1)	C(21)−Fe(2)−C(20)	89.46(18)
C(22)−Fe(2)−C(20)	90.54(18)	C(21)−Fe(2)−C(20)^{iii}	89.46(18)
C(22)−Fe(2)−C(20)^{iii}	90.54(18)	C(20)−Fe(2)−C(20)^{iii}	178.9(4)
C(21)−Fe(2)−C(23)	89.60(11)	C(22)−Fe(2)−C(23)	90.40(11)
C(20)−Fe(2)−C(23)	91.21(14)	C(20)^{iii}−Fe(2)−C(23)	88.79(14)
C(21)−Fe(2)−C(23)^{iii}	89.60(11)	C(22)−Fe(2)−C(23)^{iii}	90.40(11)
C(20)−Fe(2)−C(23)^{iii}	88.79(14)	C(20)^{iii}−Fe(2)−C(23)^{iii}	91.21(14)
C(23)−Fe(2)−C(23)^{iii}	179.2(2)		

$i = -x + {}^{3}/_{2}, y, -z + {}^{1}/_{2}$; $ii = -x + 2, -y + 1, -z + 1$; $iii = -x + {}^{3}/_{2}, y, -z + {}^{3}/_{2}$

product per Fe_2 unit for **1**, in the temperature range 2−295 K and under an applied magnetic field of 1 T. To gain insight into its magnetic behavior at very low temperature, we have studied the temperature dependence of the $\chi_M T$ product under a magnetic field of 50 G (Figure 4), thus preventing the compound from magnetic saturation. In the high-temperature range, the thermal behavior of the $\chi_M T$ product per Fe_2 is the same as that observed at 1 T. Thus, as the temperature is lowered, the $\chi_M T$ product steadily increases from room temperature, with a value of 1.06 $cm^3mol^{-1}K$, until reaching a maximum of 3.8 $cm^3mol^{-1}K$ at about 6 K, and then sharply decreases to 1.7 $cm^3mol^{-1}K$ upon cooling to 2 K. This behavior is consistent with a ferromagnetic intrachain interaction and antiferromagnetic interchain interactions, which are responsible of the decrease of $\chi_M T$ at very low temperature. The $\chi_M T$ product

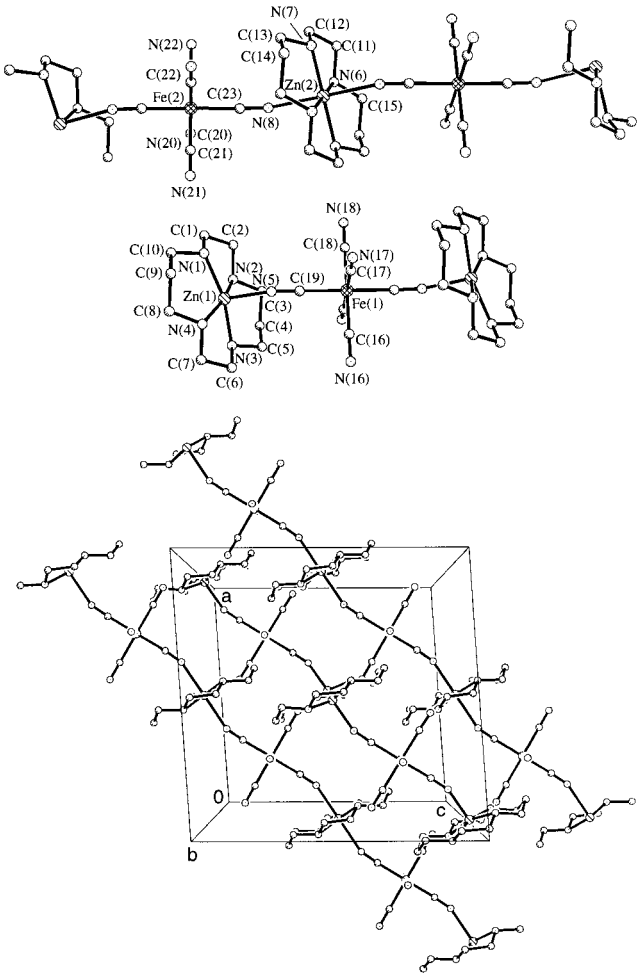

Figure 3. A perspective view of a anionic chain and a trinuclear cation with the atom labeling scheme (top) and a view of the ionic chains and trimers in the ac plane (bottom).

at room temperature is significantly larger than the spin-only value of 0.75 $cm^3mol^{-1}K$ expected for two isolated low-spin iron(III) ions ($S = 1/2$), assuming $g = 2.0$, probably because of an orbital contribution to the magnetic moment of the low-spin iron(III) ions.

The unexpected ferromagnetic interaction between the Fe(III) ions along the chain can be rationalized on the basis of the axially elongated octahedral geometry (D_{4h}) of the low spin Fe(III) ions of the $[Fe(cyclam)]^{3+}$ unit. In this geometry, the unpaired electron is located on the d_{xy} orbital of B_{2g} symmetry (see Figure 4). Thus, the interaction between this magnetic orbital and d_{xz} and d_{yz} (t_{2g}) magnetic orbitals on the almost perfect octahedral Fe(III) ion of the $[Fe(CN)_6]^{3-}$ unit leads to zero overlap and then to a ferromagnetic interaction. The delta $d_{xy}-d_{xy}$ interaction is much more reduced in magnitude and then a global ferromagnetic interaction is observed. Noteworthy, a similar unexpected ferromagnetic coupling has been also observed between $Cr(t_{2g}3)$ ions in the compound catena-cyano-(phthalocyaninato) chromium(III).[35]

Antiferromagnetic interchain interactions through an intricate network of hydrogen bonds leads to an antiferromagnetic ordering at 5.5 K, which is supported by the maximum in the in phase ac magnetic susceptibility at 5.5 K and by the maximum in the M vs T curve (Figure 5). This maximum broadens and shifts to lower temperatures as the magnetic field increases and

(35) Schwartz, M.; Hatfield, W. E.; Joesten, M. D.; Hanack, M.; Datz, A. *Inorg. Chem.* **1985**, *24*, 4198.

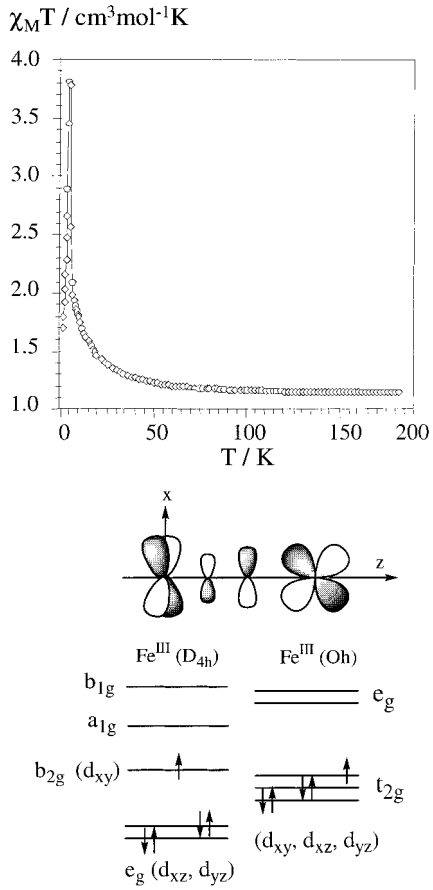

Figure 4. $\chi_M T$ vs T (top) and electronic configuration of the metal centers (bottom) for **1**.

finally disappears for $H > 1$ T. This behavior points out the existence of a field-induced transition from an antiferromagnetic ground state to a ferromagnetic state and so **1** is a metamagnet with a critical field of 1 T. The (M/Nβ) vs H curve at 2 K is sigmoidal and typical of a metamagnet and, as expected, for $H > 1$ T it exhibits hysteresis (Figure 5). The value of magnetization at the maximum applied field of 5 T is 2.1 Nβ, which agrees well with the expected $S = 1$ value of 2.0 Nβ (with $g_{Fe1} = g_{Fe2} = 2.00$) for the saturation magnetization of two ferromagnetically coupled low spin Fe(III) ions. At 2 K and applied fields lower that the critical field, the magnetization vs H curve exhibits a very small hysteresis loop with a remnant magnetization of 0.003 Nβ and a coercitive field of 50 G. This fact points out the existence of a net magnetic moment in the antiferromagnetic phase, more likely due to spin canting of the local Fe(III) spins, which is responsible of the out-of-phase signal, χ''_{ac}, in the ac dynamic susceptibility vs T plot (Figure 5).

The temperature dependence of the $\chi_M T$ product per Mn_2Ni_3 unit in the range 2−300 K for **3**, under an applied field of 0.1 T, is shown in Figure 6. The $\chi_M T$ product increases smoothly from room temperature until 25 K and then sharply with decreasing temperature, reaching a maximum value of 20.5 emu.mol^{-1}K at 16 K. Below this temperature $\chi_M T$ decreases on cooling to 2 K. This behavior is consistent with an intralayer ferromagnetic interaction between Mn(III) and Ni(II), due to the strict orthogonality of the magnetic orbitals of the Mn(III) ($t_{2g}4$) and Ni(II) ($t_{2g}6e_g2$), and antiferromagnetic interlayers interactions. The χ_M vs T plot (inset of Figure 6) exhibits a maximum at 16 K, which clearly indicates that interlayers interactions lead to an antiferromagnetic ordering. This is also supported by the absence of an out-of-phase signal in the *ac* susceptibility vs T curve (see below). As for **2**, the (M/Nβ) vs H curve at 1.9 K (Figure 6) is sigmoidal and typical of a metamagnet with a critical field of 1 T. At 2 K and applied magnetic fields upper than the critical field, the compound behaves as a typical ferromagnet and, consequently, the (M/Nβ) vs H curve exhibits hysteresis loop with a remnant

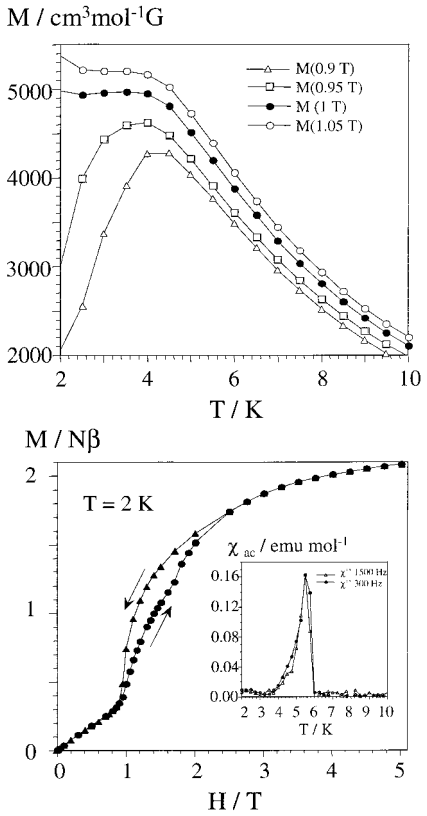

Figure 5. M vs T (top), M vs H (bottom) and χ''_{ac} vs T (inset-bottom) for **1**.

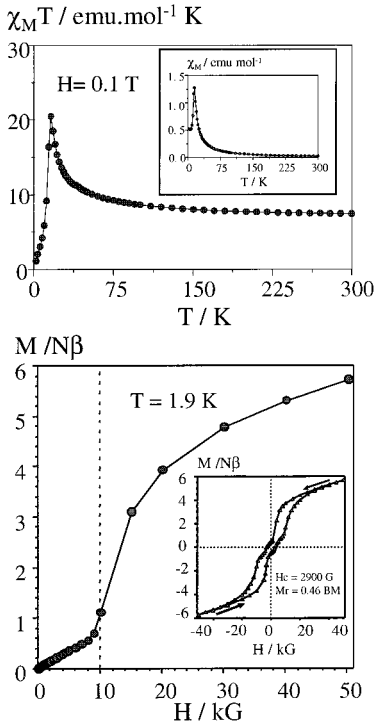

Figure 6. $\chi_M T$ vs T (χ_M vs T, inset) at $H = 0.1$ T (top), M vs H (bottom) and hysteresis curve (inset-bottom) for **3**.

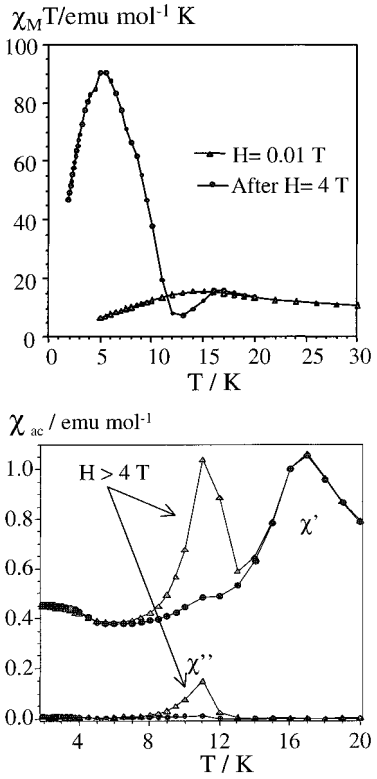

Figure 7. $\chi_M T$ vs T (top) and χ_{ac} vs T (bottom) for **3**.

magnetization of 0.46 Nβ per Ni_3Mn_2 unit and a very significant coercitive field of 2900 G, which is typical of hard ferromagnets (inset Figure 6). On increasing temperature to 5 K, the remanent magnetization and coercitive field decrease to 0.35 Nβ and 1000 G, respectively, as expected. When the compound is placed at 2 K under a magnetic field of 5 T and then the field is switched off, the field-induced magnetization remains constant with the time, indicating a good memory effect for this material. If in these conditions, the magnetic field is switched on at 100 G and the magnetic susceptibility is measured from 2.0 K to room temperature (Figure 7), the $\chi_M T$ product increases linearly with increasing temperature, reaching a maximum value of 90 emu·mol^{-1}K at about 9 K. This behavior clearly indicates that the compound is magnetically saturated in the 2−9 K temperature range. Above 9−10 K, $\chi_M T$ rapidly decreases and the compound is going into the antiferromagnetic phase. This behavior is very well observed in the in phase, χ'_{ac}, and out-of-phase, χ''_{ac}, ac dynamic susceptibilities vs. temperature plots (Figure 7). The χ'_{ac} curve shows only one signal with maximum at 16K, which is due to the antiferromagntic ordering. Consequently, the χ''_{ac} vs T plot does not exhibits any signal. However, when **3** is placed within an applied magnetic field of 4 T and then the field is switched off, the χ'_{ac} curve exhibits two signals, one due to the antiferromagnetic ordering at 16 K and a new one with a maximum at 11 K due to a ferromagnetic ordering. The χ''_{ac} vs T plot exhibits a maximum, which is not frequency dependent, at 11 K, thus confirming the ferromagnetic nature of the magnetic ordering. The above results clearly point out that if the compound is placed in a magnetic field higher than the critical field (in the ferromagnetic phase) and then the field is switched off, the compound will exhibits a field-induced magnetization below $T_c = 11$ K.

All these magnetic data confirm that **3** has essentially the same metamagnetic character of **2**. However, the isostructural substitution of $[Fe(CN)_6]^{3-}$ by $[Mn(CN)_6]^{3-}$ leads to important differences. First, T_N moves from 7.7 K in **2**[10] to 16 K in **3** as

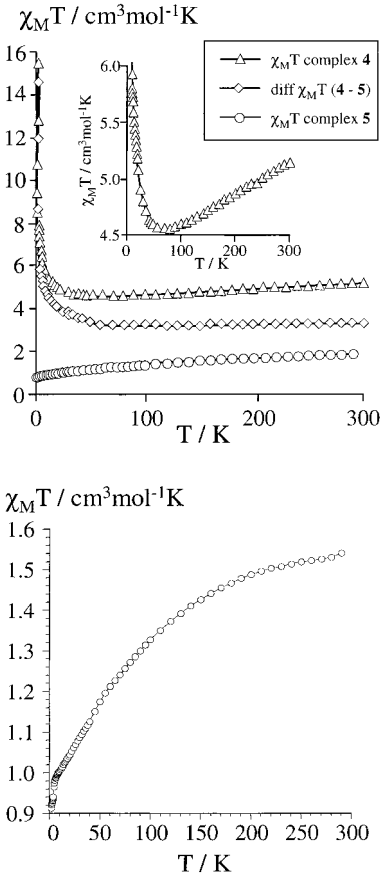

Figure 8. $\chi_M T$ vs T for **4** (top) and a plot of the difference in $\chi_M T$ between **4** and **5** in order to eliminate the spin−orbit contribution belonging to the LS Fe^{III} ions (bottom).

a consequence of the increase of the magnetic exchange interaction as the number of t_{2g} electrons increases. In keeping with this, the same isostructural substitution in the compound $[K\{Mn(3\text{-}MeOsalen)\}_2\{Fe(CN)_6\}]_n$[36] promotes an increase in T_N from 9.2 to 16 K. Second, and more important, the coercitivity dramatically increases from **2** to **3** due to the magnetic anisotropy of the Mn(III) ion, with an orbitally degenerate $^3T_{1g}$ ground state, which prevents the domains from rotating freely when the field is applied.

The temperature dependence of the $\chi_M T$ product per Fe_2Ni_3 for **4** is given in the Figure 6. As can be observed in this figure, the $\chi_M T$ decreases with decreasing temperature reaching a minimum at about 60 K. Such a magnetic behavior is characteristic of a low-spin octahedral iron(III) system with spin−orbit coupling of the $^2T_{2g}$ ground term. In fact, when the $\chi_M T$ product between 60 K and room temperature for compound **5**, whose magnetic properties are essentially due to isolated iron(III) ions of the $[Fe(CN)_6]^{3-}$ units, is subtracted from the $\chi_M T$ vs T curve for **4**, the resulting $\chi_M T$ remains almost constant in this temperature range with the value expected for three isolated Ni(II) ions. This result confirms that the magnetic behavior of **4** in the high-temperature range is due to spin−orbit coupling effects. Below 60 K the $\chi_M T$ continuously increases on cooling to 2 K, thus indicating a ferromagnetic exchange interaction between Fe(III) and Ni(II) ions within the layer, as a consequence of the strict orthogonality of their magnetic orbitals. Noteworthy, in this case does appear neither a maximum in the χ_M vs T curve nor an out-of-phase signal in the ac susceptibility,

(36) Re, N.; Gallo, E.; Floriani, C.; Miyasaki, H.; Matsumoto, N. *Inorg. Chem.* **1996**, *35*, 5964.

which would indicate antiferromagnetic and ferromagnetic orderings above 2 K, respectively. This behavior may be due to the increase in the interlayers separation for **4** when compared to **2**, which may be promoted, at least in part, by the methyl groups of the macrocyclic ligand.

For **5**, $\chi_M T$ steadily decreases with decreasing temperature reaching a value of 1.0 emu·mol^{-1}K at 10 K (Figure 8). This behavior is due to the spin−orbit coupling effect of the low spin iron(III) ions. In fact, the difference in $\chi_M T$ between room temperature and 10 K, is just twice that observed for the linear chain compound K[Cu(cyclam)][Fe(CN)$_6$]·4H$_2$O,[9] which contains only one hexacyanoferrate(III) unit. Below 10 K, $\chi_M T$ decreases sharply, which may be due to the combined effect of the intrachain and interchain exchange interactions.

Concluding Remarks

The 1D linear chain compound, [Fe(cyclam)][Fe(CN)$_6$]·6H$_2$O **1**, exhibits a metamagnet behavior with a Neel temperature T_N = 5.5 K and a critical field at 2 K of 1 T, where the ferromagnetic interaction operates within the chain and the antiferromagnetic one between chains. The unexpected ferromagnetic interaction between iron(III) ions along the chain can be rationalized on the basis of the axially elongated octahedral geometry of the low spin Fe^{III} ions of the [Fe(cyclam)]$^{3+}$ unit, leading to orthogonality between the d_{xy} magnetic orbital of this unit and the d_{xz} and d_{yz} magnetic orbitals of the almost perfect octahedral [Fe(CN)$_6$]$^{3-}$ unit. Noteworthy, at 2 K and H < 1 T this compound exhibits a net magnetic moment, which is likely due spin canting of the iron(III) local spins. The isostructural substitution of [Fe(CN)$_6$]$^{3-}$ by [Mn(CN)$_6$]$^{3-}$ in [Ni(cyclam)]$_3$[Fe(CN)$_6$]$_2$·12H$_2$O **2**, leads to [Ni(cyclam)]$_3$[Mn(CN)$_6$]$_2$·16 H$_2$O **3**, which exhibits a corrugated 2D honeycomblike structure a metamagnet with T_N = 16 K and a critical field of 1 T. However, the isostructural substitution of [Fe(CN)$_6$]$^{3-}$ by [Mn(CN)$_6$]$^{3-}$ leads to important differences. First, T_N moves from 7.7 K in **2** to 16 K in **3** as a consequence of the increase of the magnetic exchange interaction as the number of t_{2g} electrons increases. Second, and more important, the coercitivity dramatically increases from **2** to **3** due to the magnetic anisotropy of the Mn(III) ion, with an orbitally degenerate $^3T_{1g}$ ground state, which prevents the domains from rotating freely when the field is applied.

Although complex [Ni(CTH)]$_3$[Fe(CN)$_6$]$_2$·13H$_2$O **4** also has a corrugated 2D honeycomblike structure and ferromagnetic intralayer interaction, however in contrast to **2** and **3,** does exhibits neither a maximum in the χ_M vs T curve, which would indicate an antiferromagnetic ordering, nor an out-of-phase signal in the ac susceptibility indicative of a ferromagnetic ordering. This behavior may be due to the increase in the interlayers separation for **4** when compared to **2**.

The fact that the [Zn(cyclam)]$^{2+}$ unit can accept one or two nitrogen atoms of the bridging cyanide groups in axial positions, leading to ZnN$_5$ and ZnN$_6$ chromophores, allows the formation of a new structural type in **5**. Its unique structure consists of polymeric anionic chains of alternating [Zn(cyclam)]$^{2+}$ and [Fe(CN)$_6$]$^{3-}$ units along the crystallographic *c* axis and cationic trinuclear entities, [Zn(cyclam)Fe(CN)$_6$Zn(cyclam)], that compensate charge. Their magnetic properties agree well with those expected for two isolated [Fe(CN)$_6$]$^{3-}$ unit with spin−orbit coupling effect of the low spin iron(III) ion.

Acknowledgment. This study was financially supported by the Dirección General de Investigación Científica y Técnica (Spanish Government, Grant N×bc PB97/0822) and Junta de Andalucia.

Supporting Information Available: Two crystallographic files in CIF. This material is available free of charge via Internet at http://pubs.acs.org.

IC0103446